
JOURNAL OF THE AMERICAN CHEMICAL SOCIETY

Early Intermediates in Spermidine-Induced DNA Condensation on the Surface of Mica

Ye Fang and Jan H. Hoh*

Contribution from the Department of Physiology, Johns Hopkins University School of Medicine, 725 North Wolfe Street, Baltimore, Maryland 21205

Received April 20, 1998

Abstract: The folding pathway of spermidine-induced DNA condensation on the surface of mica was examined by varying the concentration of spermidine in a dilute DNA solution and visualizing intermediates by atomic force microscopy (AFM). Images reveal that spermidine-induced DNA condensation on mica involves multiple well-defined structural intermediates. At 1.5–3 μM spermidine there are no interesting morphologies of the DNA, although there is a reduction of the apparent persistence length. At 7.5–15 μM spermidine, intramolecular loops (mean diameter 40 ± 15 nm) form. Loops initially appear to form independently of each other, but individual molecules with multiple loops tend to crossover at the same point producing “flower”-shaped structures. At 30 μM spermidine, the tendency to form single crossover points increases and multimolecular flowers form. After initial flower formation disklike condensates appear, sometimes as apparent outgrowths from flowers. The resolvable strands in the disks are thicker than double-stranded DNA, suggesting a close association of two or more DNA strands and, thus, a stabilization of strand–strand interactions along the length of the DNA. This strand–strand stabilization is further indicated by the formation of very large (> 500 nm) multimolecular aggregates, at 150 μM spermidine, composed predominantly of flowers and disks. These aggregates are initially planar with a monomolecular thickness and few crossover points. At the highest spermidine concentrations examined growth in the third dimension is seen as additional layers of condensates formed. These results suggest that there are several intermediates early in spermidine-induced DNA condensation on mica, with well-defined characteristics. Some of these intermediates have novel intra- and intermolecular contacts.

Introduction

Large DNA molecules are highly condensed in viral capsids and in the nuclei of eukaryotic cells. The condensed phase DNA must be highly organized to maintain stability of the genome and allow replication to proceed in an orderly manner. Further, the regulation of DNA condensation and decondensation is important for protecting and repressing genetic information during the replicative cycles of organisms ranging from viruses

to higher eukaryotes.¹ DNA condensation can accelerate a number of biologically relevant processes, such as DNA strand-exchange and renaturation,^{2,3} ligation,⁴ and catenation of closed circular DNA.⁵ In addition, there are general approaches to nonviral gene therapy that require the controllable condensation of DNA vectors containing specific functional genes into

* Corresponding author. Phone: +1-410-614-3795. Fax: +1-410-614-3797. E-mail: jan.hoh@jhu.edu.

(1) van Holde, K. E. *Chromatin*; Springer-Verlag: New York, 1988.
(2) Camerini-Otero, R. D.; Hsieh, P. *Cell* **1993**, *73*, 217.
(3) Sikorav, J. L.; Church, G. M. *J. Mol. Biol.* **1993**, *222*, 1085.
(4) Zimmerman, S. B.; Harrison, B. *Proc. Natl. Acad. Sci. U.S.A.* **1987**, *84*, 1871.
(5) Krasnow, M. A.; Cozzarelli, N. R. *J. Biol. Chem.* **1982**, *257*, 2687.

particles with well-defined properties.^{6,7} The importance of controlling the condensation of DNA containing functional genes has been highlighted by recent investigations, which show that the transfection efficiency generally correlates to the packing density and order of condensed phase DNA.^{8,9} Thus, the molecular mechanisms of DNA condensation are of considerable importance.

DNA condensation in vitro has been considered an important model system for understanding the dense, higher ordered structures that DNA can form in vivo. One of the most widely studied systems for in vitro DNA condensation is the formation of well-defined structures, in particular toroids and rods, in the presence of multivalent cations.^{10–12} This system is thought to be biologically relevant,^{10,11} and toroids formed by multivalent cations appear structurally similar to the phage DNA in the precursor capsids of viruses.¹³ In vitro, toroids and rods are typically formed by simple mixing of a dilute DNA solution with a multivalent cation such as spermidine or $\text{Co}(\text{NH}_3)_6^{3+}$.^{10–12} The resulting condensates have been characterized extensively by a variety of methods, and their structure is well defined.^{14–19} In addition, the thermodynamics of the condensation process have been described in some detail.^{20–23} Recent work on the structure of toroids has focused on models for how the DNA is wound within the toroid, for which there are two models, the spool model²⁴ and the constant loop model.²⁵ However, with the exception of a recent report from Böttcher et al.,²⁴ there are no known structural intermediates during the formation of these types of DNA condensates. The condensation intermediates reported by Böttcher et al.²⁴ are formed in the presence of spermine and uranyl acetate and are complex multimolecular structures that are characterized by parallel bundles of DNA with frequent partial toroids. Hence these appear to be relatively late intermediates. Here we describe a series of structures with well-defined characteristics formed using varying concentrations of spermidine and adsorption to mica. These structures are stable on the time scale of minutes to hours and appear to be early intermediates in a condensation pathway.

(6) Felgner, P. L.; Gadek, T. R.; Holm, M.; Roman, R.; Chan, H. W.; Wenz, M.; Northrop, J. P.; Ringold, G. M.; Danielsen, M. *Proc. Natl. Acad. Sci. U.S.A.* **1987**, *84*, 7413.

(7) Lasic, D. D. *Liposomes in Gene Delivery*; CRC Press: Boca Raton, FL, 1997.

(8) Radler, J. O.; Koltover, I.; Salditt, T.; Safinya, C. R. *Science* **1997**, *275*, 810.

(9) Niidome, T.; Ohmori, N.; Ichinose, A.; Wada, A.; Mihara, H.; Hirayama, T.; Aoyagi, H. *J. Biol. Chem.* **1997**, *272*, 15307.

(10) Bloomfield, V. A. *Biopolymers* **1991**, *31*, 1471.

(11) Bloomfield, V. A. *Curr. Opin. Struct. Biol.* **1996**, *6*, 334.

(12) Marquet, R.; Houssier, C. *J. Biomol. Struct. Dyn.* **1991**, *9*, 159.

(13) Cerritelli, M. E.; Cheng, N.; Rosenberg, A. H.; McPherson, C. E.; Booy, F. P.; Steven, A. C. *Cell* **1997**, *91*, 271.

(14) Chatteraj, D. K.; Gosule, L. C.; Schellman, J. A. *J. Mol. Biol.* **1978**, *121*, 327.

(15) Gosule, L. C.; Schellman, J. A. *Nature* **1976**, *259*, 333.

(16) Marx, K. A.; Ruben, G. C. *Nucleic Acids Res.* **1983**, *11*, 1839.

(17) Eickbush, T. H.; Moudrianakis, E. N. *Cell* **1976**, *13*, 295.

(18) Arscott, P. G.; Ma, C.; Wenner, J.; Bloomfield, V. A. *Biopolymers* **1995**, *36*, 345.

(19) Allen, M. J.; Bradbury, E. M.; Balhorn, R. *Nucleic Acids Res.* **1997**, *25*, 2221.

(20) Widom, J.; Baldwin, R. L. *Biopolymers* **1983**, *22*, 1595.

(21) Porschke, D. *Biochemistry* **1983**, *23*, 4821.

(22) Melnikov, S. M.; Sergeyev, V. G.; Yoshikawa, K. *J. Am. Chem. Soc.* **1995**, *117*, 2401.

(23) Yoshikawa, K.; Takahashi, M.; Vasilevskaya, V. V.; Khokhlov, A. R. *Phys. Rev. Lett.* **1996**, *76*, 3029.

(24) Böttcher, C.; Endiskh, C.; Fuhrhop, J.-H.; Catterall, C.; Eaton, M. *J. Am. Chem. Soc.* **1998**, *120*, 12.

(25) Hud, N. V.; Downing, K. H.; Balhorn, R. *Proc. Natl. Acad. Sci. U.S.A.* **1995**, *92*, 3581.

Experimental Section

DNA and Chemicals. All experiments were performed using a 3033-base pair (bp) plasmid pSP64 poly(A) (Boehringer-Mannheim, Indianapolis, IN), linearized by completely digestion with the *ScaI* endonuclease (Boehringer-Mannheim). Following linearization the DNA fragment was purified using Gene Clean (Bio101, Vista, CA) and precipitation with ethanol. The DNA pellet obtained was resuspended in Millipore purified water ($>18 \text{ M}\Omega \text{ cm}^{-1}$; MilliQ-UV, Millipore Co., Bedford, MA) and stored at -20°C . DNA concentration was determined by the absorption at 260 nm and is reported here in terms of moles of molecules. Salts were used as received from Sigma Chemical Co. (St. Louis, MO).

Sample Adsorption. Nine millimeter diameter disks of ruby muscovite mica (grade V1-V2; Asheville-Schoemaker Mica Co., Newport News, VA), each attached to a magnetic steel disk, were used as substrates for DNA adsorption. All experiments were performed by mixing an equal volume of a 1 nM DNA solution and a spermidine solution of appropriate concentration. Samples were incubated at room temperature for 30 min. A 20- μL aliquot of the mixture was deposited onto freshly cleaved mica and incubated for 5 min in a humidified chamber. The samples were rapidly blow dried using a burst of compressed gas (Vari-Air, Peca Products, Janesville, WI). Attempts to rinse the samples with water prior to drying were unsuccessful, apparently as a result of very rapid decondensation. This limited the highest concentration used to 150 μM spermidine, with higher concentrations interfering with the AFM imaging.

To examine the stability of intermediates in solution, equal volumes of 1 nM DNA and 60 μM spermidine were mixed and incubated at room temperature for 1, 6, 26, 56, and 116 min. A 20- μL aliquot was deposited onto freshly cleaved mica and incubated for an additional 4 min and then dried as above. To examine substrate effects on the condensation process, a 1 nM DNA solution was mixed with an equal volume of 100 μM spermidine and incubated at room temperature for 2 h. A 20- μL aliquot was deposited onto freshly cleaved mica, incubated for varying lengths of time, and then blown dry.

AFM Imaging. A Nanoscope IIIa AFM controller with a Multi-mode AFM (Digital Instruments, Santa Barbara, CA) was used for imaging. Single-crystal silicon cantilevers (Model TESP; Digital Instruments) were cleaned by exposure to high-intensity UV light (UVO-Cleaner, Jelight Co. Inc., Laguna Hills, CA) for 3 min before use. All AFM imaging was conventional ambient tapping mode AFM, with scan speeds of about 5 Hz and data collection at 512×512 pixels. All images are shown with inverted contrast so that those darker features are taller than lighter features. Most of the AFM images were taken at a scan size of $3 \mu\text{m} \times 3 \mu\text{m}$.

Data Processing. The AFM data were analyzed using AFMIPS and NIH Image. AFMIPS is an analysis tool developed in our laboratory that can automatically outline DNA molecules and determine their contour lengths.^{26,27} The AFMIPS was used in a semi-interactive mode where all the output from the program were monitored and occasionally checked manually by the operator. For the present work an additional function was added for the persistence length measurements. Nanoscope AFM files were over sampled approximately 40-fold by a polynomial interpolation. To determine the persistence length the angle θ between two segments separated by a distance l was measured and subjected to moment analysis as previously described.²⁸ Where needed, hand tracing of DNA molecules was performed using NIH Image (Version 1.58 or later). Loop sizes were determined by measuring the loop contour length and dividing this value by π .

Results

The experimental approach used here was to move DNA along a condensation pathway by gradually increasing the concentration of spermidine and examining structures that

(26) Fang, Y.; Spisz, T. S.; Wiltshire, T.; D'Costa, N. P.; Bankman, I. N.; Reeves, R. H.; Hoh, J. H. *Anal. Chem.* **1998**, *70*, 2123.

(27) Spisz, T. S.; Fang, Y.; Seymour, C. K.; Reeves, R. H.; Hoh, J. H.; Bankman, I. N. *Med. Biol. Eng. Comput.* **1998**, in press.

(28) Frontali, C.; Dore, E.; Ferrauto, A.; Gratton, E. *Biopolymers* **1979**, *18*, 1353.

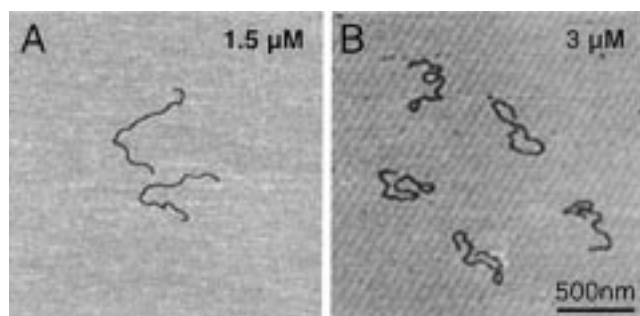


Figure 1. Representative AFM images of DNA in the presence of (a) 1.5 μM and (b) 3.0 μM spermidine.

Table 1. Distribution of Extended and Looped DNA Molecules in the Presence of Low Concentrations of Spermidine^a

$C_{\text{spermidine}}$ (μM)	extended (%)	single- looped (%)	double- looped (%)	multilooped (%)	N_{total}
0 ^b	91	7	2	0	170
3.0	72	22	4	2	92
7.5	14	38	23	25	240
15	6	12	22	60	150

^a $C_{\text{spermidine}}$ is the concentration of spermidine, and N_{total} is the number of molecules analyzed. The total number of AFM images examined were 25, 25, 15, and 10 for 0, 3, 7.5, and 15 μM spermidine, respectively. ^b 5 mM MgCl_2 was used to promote adsorption.

formed on the time scale of minutes to hours by adsorption to mica and AFM imaging. Thus the results are presented as representative images at increasing spermidine concentrations, with qualitative or quantitative analysis of the intermediates where appropriate. In addition the stability of some intermediates was examined by varying incubation times with spermidine and adsorption times on the mica.

Structures Observed at 1.5–3 μM Spermidine. At the lowest spermidine concentrations examined, the morphologies of the DNA molecules on the surface appear unremarkable. The molecules are linear with rare intermolecular or intramolecular contacts (Figure 1 and Table 1), and there are no obvious morphological differences when compared to those of the control DNA adsorbed in the absence of spermidine. The controls used were adsorbed in the presence of 5 mM MgCl_2 because DNA does not adsorb well to the mica substrate in pure water. There is a decrease in the apparent persistence length from 102 nm for the control DNA to 52 nm for DNA in the presence of 3 μM spermidine, as determined using the method of Frontali et al.²⁸ Note that for the relatively large 3-kb DNA used there are excluded volume effects that increase the apparent persistence length.²⁹

Structures observed at 7.5–15 μM spermidine. In this range of spermidine concentrations, distinct morphologies of DNA molecules are observed (Figure 2). At 7.5 μM spermidine a large fraction (86%) of molecules have at least one intramolecular loop (Table 1). The mean diameter of this loop is 40 ± 15 nm (Figure 3). The persistence length (48 nm) is essentially identical to that at 3 μM spermidine. As the concentration of spermidine is increased to 15 μM , the number of loops increases, although they are still predominantly intramolecular. Many molecules have two or more independent loops (e.g., Figure 2B,C), although other molecules with multiple intramolecular loops that cross at a single point can also be seen (Figure 2D). These latter structures gives rise to a class of structures we call “flowers.”

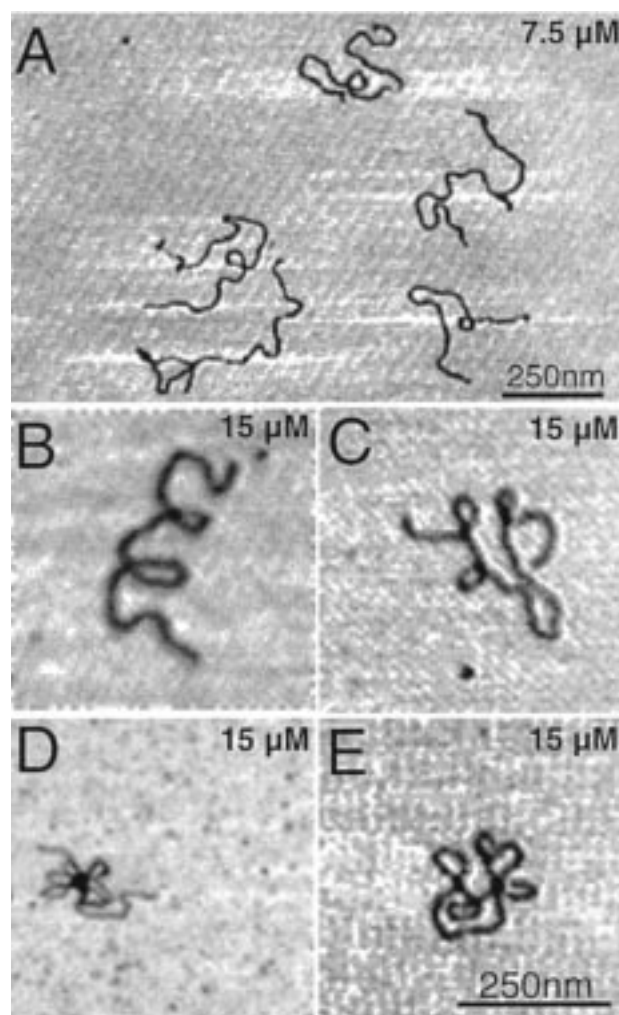


Figure 2. Representative AFM images of DNA in the presence of 7.5–15 μM spermidine. (a) A significant fraction of the DNA molecules have single loops in the presence of 7.5 μM spermidine, while (b–e) structures with more than one loop in a single DNA molecule were formed in the presence of 15 μM spermidine. Many of the loops at this concentration were apparently independent of each other, although some loops shared a common crossover point.

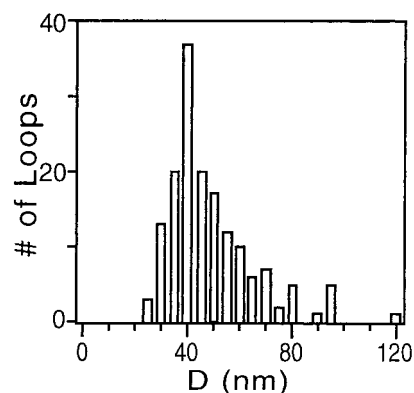


Figure 3. Distribution of the diameters of the individual loops formed at 7.5 μM spermidine. Similar results are obtained at 15 μM spermidine (not shown).

Structures observed at 30 μM spermidine. Flowers become very prevalent as the spermidine concentration is further increased. The structures observed at 30 μM are characterized by being to a large extent multimolecular structures (Figure 4). This is in many cases obvious from a visual inspection and

(29) Rivetti, C.; Guthold, M.; Bustamante, C. *J. Mol. Biol.* **1996**, *264*, 919.

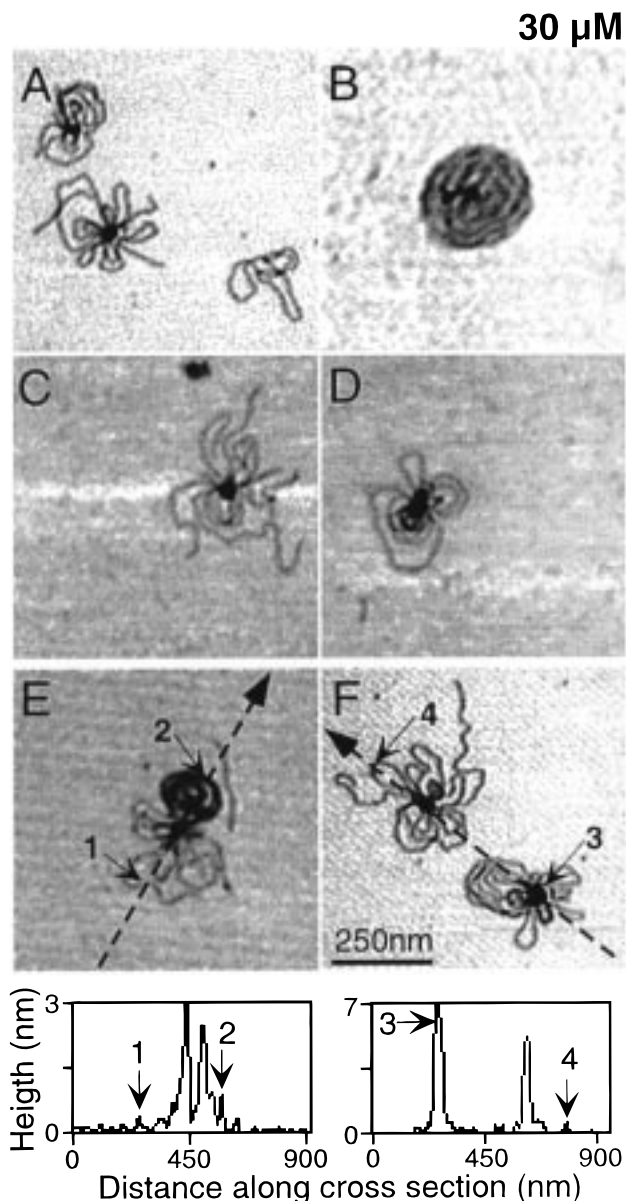


Figure 4. Representative AFM images of DNA in the presence of 30 μM spermidine. (a, c–f) The most striking features are multimolecular flower-shaped structures, which all have one or few crossover points. Cross sections shown below panels e and f show that the crossover points are as much as 5–10 times taller than that of a single double-stranded DNA molecule. Note that double-stranded DNA imaged by ambient tapping mode is well-known to appear much thinner than expected, in this case <1 nm. (b) A disk-shaped condensate also appears at this spermidine concentration.

knowing that the length of a single molecule is ~ 1 μm . It can also be confirmed by very approximate hand tracing of molecules (not shown) or the presence of more than two free ends in a structure. The multimolecular flowers generally have a single crossover point, which appears as a very tall structure with a height (measured from the cross section) often 5–10 times taller than an isolated DNA strand. In some larger structures there are multiple crossover points, although they are rare. Another structure which is roughly circular, and hence called a “disk”, also appears. The thickness of the strands within a disk is usually greater than those in the flowers, suggesting that the strands in a disk are composed of at least two closely associated DNA strands. In some aggregates it appears as though a disk is forming from a nested set of loops in a multimolecular flower (e.g., Figure 4E).

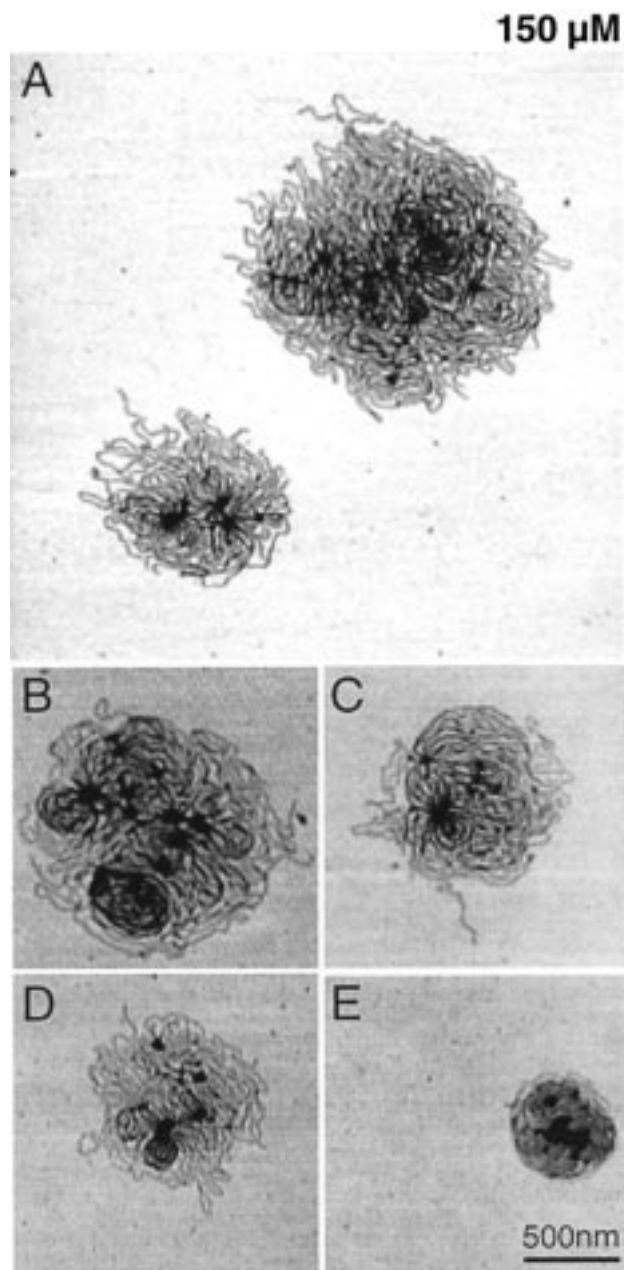


Figure 5. Representative AFM images of DNA in the presence of 150 μM spermidine. (a–e) At the highest spermidine concentrations examined extremely large multimolecular aggregates of the DNA are seen. These aggregates are largely planar with relatively few crossover points.

Structures Observed at 150 μM spermidine. At the highest concentrations of spermidine examined, the structures formed become extremely large and complex and, in some cases, must be composed of hundreds of DNA molecules (Figure 5). Single DNA molecules well separated from the aggregates, either relaxed or condensed, are extremely rare. Flower-like structures and disks are seen in these complex structures. Many of the condensates are so large that they apparently present a new surface for additional condensation, resulting in a layer of condensed structures on top of another. It is very difficult to trace out any exact paths in the DNA in these structures, and thus, the relationship between structures laying on top of each other cannot be determined. The number of crossover points remains relatively small. In fact, in some aggregates, it appears that the crossover points have come close together and begun

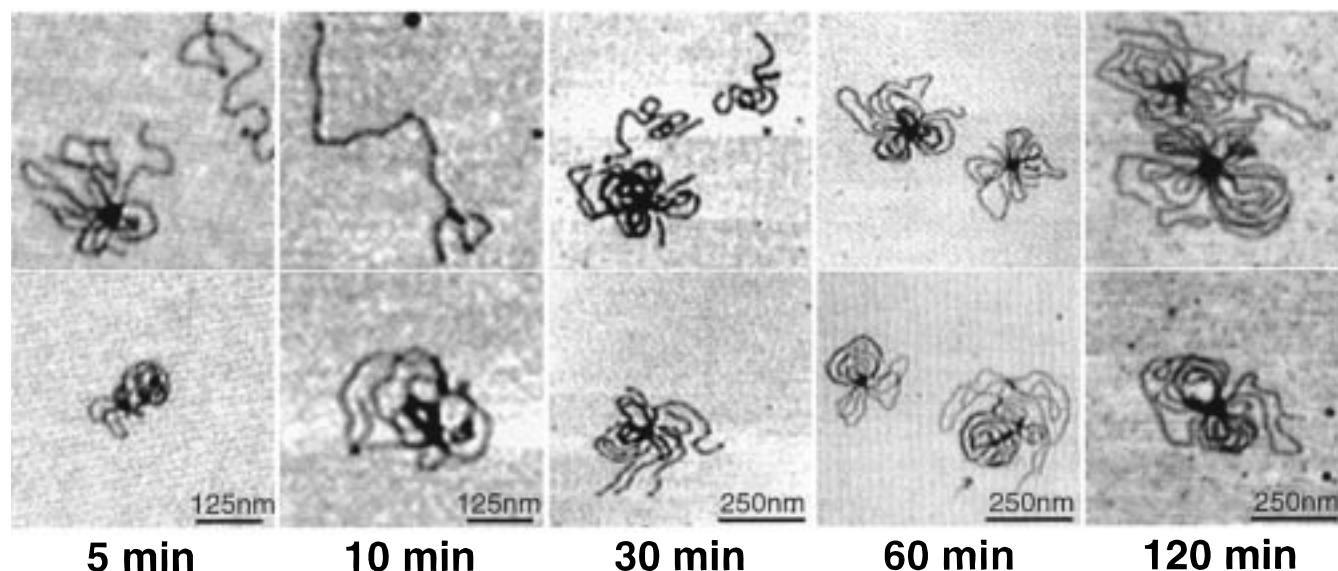


Figure 6. Effect of incubation time in solution on the formation of condensates. DNA incubated with $30 \mu\text{M}$ spermidine for increasing lengths of time prior to adsorption showed some variability in structures during the first 30 min. Beyond 30 min the structures appeared stable for up to 2 h. All adsorptions were 4 min.

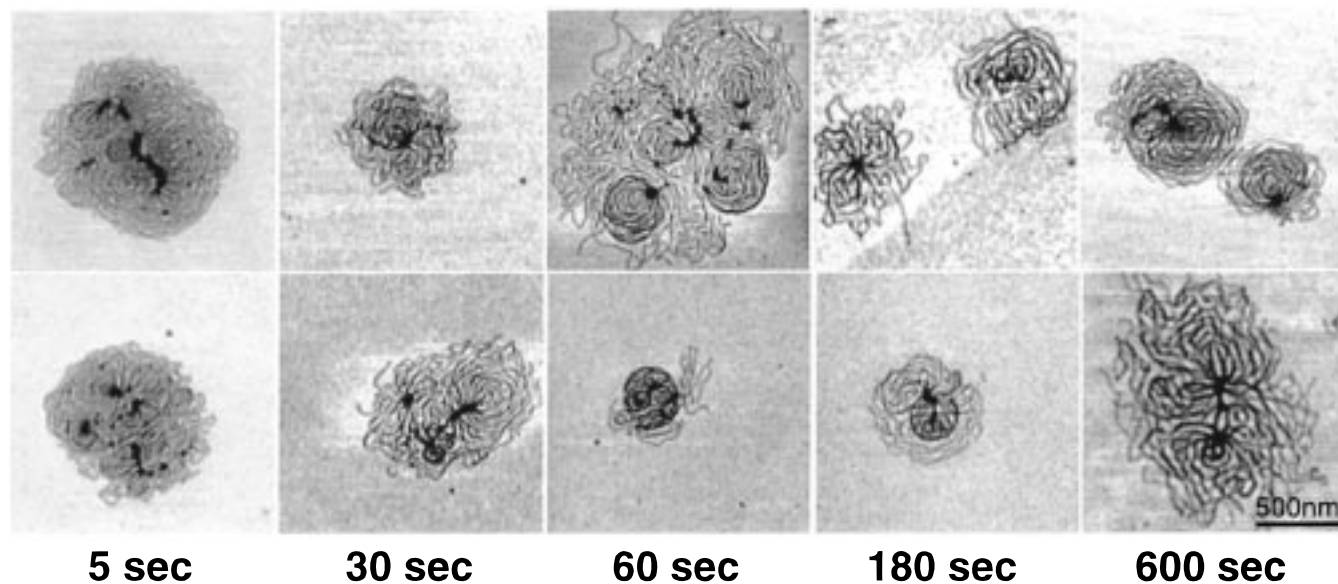


Figure 7. Effect of adsorption time on the formation of condensates. DNA was incubated at $50 \mu\text{M}$ for 2 h in solution and then adsorbed for varying lengths of time as shown in the figure. No significant effects of the adsorption to mica over this time scale are evident.

to form rodlike structure. Spermidine at $150 \mu\text{M}$ was the highest concentration for which interpretable data was obtained. At higher concentrations the dried spermidine interfered with the imaging. Rinsing with water for even a few seconds to remove excess spermidine produced mostly relaxed molecules, suggesting that the decondensation was rapid relative to the wash time.

Stability of Intermediates in Solution. To assess the stability of some complexes over the time scale of the manipulations performed here, DNA was incubated in $30 \mu\text{M}$ spermidine for varying lengths of time, adsorbed to mica for a fixed length of time (4 min), and imaged (Figure 6). The results show that there is some variability in morphology in the first 30 min of incubation, after which the structures change more slowly or not at all.

Effect of Incubation on Mica. To investigate the effect of the substrate on the condensation process, DNA was incubated at $50 \mu\text{M}$ spermidine for 2 h and then adsorbed to mica for

varying lengths of time ranging from 5 s to 10 min (Figure 7). In this time frame there were no obvious changes in the structure of the condensates.

Discussion

Characteristics of Spermidine-Induced Condensation Intermediates on Mica. The initial step in the spermidine-induced condensation identified here is a mechanical relaxation or increased intrinsic bending of the molecule that results in a decrease of the apparent persistence length. At present it is not possible to distinguish between the relaxation- and bending-based mechanisms for this effect. However, because later structures are heavily bent, some favor is given to the idea of increased intrinsic bending of DNA at low spermidine concentration. This is also supported by the recent theoretical work of Rouzina and Bloomfield³⁰ showing that that small multivalent cations can induce local bends in DNA.

(30) Rouzina, I.; Bloomfield, V. A. *Biophys. J.* **1998**, *74*, 3152.

The next identifiable step in the process is the initial intramolecular loop formation and the stabilization of crossover points. It is counter-intuitive that single loops with an average diameter of 40 nm would be stable. However, the very high fraction of molecules with single loops at low spermidine concentration and the subsequent formation of intramolecular and intermolecular "flowers" suggests that this is a true intermediate. The diameter of the loops is remarkably close to that of conventional toroids. A priori a single loop could result from the local bending of the DNA to a certain radius of curvature, with a crossover being the result of collapsing a bent structure onto a surface. Alternatively, the loop could form by direct stabilization of a crossover point in the absence of any intrinsic bending. In either case the crossover point is clearly special in some way, since the subsequent loops formed in multimolecular flowers formed at $\geq 30 \mu\text{M}$ spermidine tend to cross at one or a few points. The crossover is thus a unique intra- and intermolecular contact point. Another interesting feature about the initial looping is that at many of the crossover points the DNA strands are nearly normal to each other. Thus it does not appear that there is significant DNA strand-strand stabilization along the length of the strands early in the condensation pathway.

Following the intramolecular loop formation, multimeric condensates appear, which require intermolecular contacts. One of those intermolecular contacts is the crossover point described above. In addition there may be interactions that involve the ends of DNA molecules. There are frequently several free ends in multimolecular condensates (e.g., Figure 4C), while other condensates have no obvious free ends (e.g., Figure 4D). In the case when there are no or few free ends there must be intra- or intermolecular contacts involving the ends. There are several possibilities for such a contact, including partial overlaps between molecules, end-to-end interactions, or termination of free ends at the crossover point. From the current data it is not possible to determine which, if any, of these types of interaction occur.

In conjunction with the multimerization of intermediates there is a stabilization of DNA strand-strand contacts along the lengths of the strands. This results in the formation of very large planar aggregates, layering of planar condensates on top of each other, and appearance of thick strands in disks. The formation of very large aggregates that are composed of loosely associated molecules and mostly monomolecular in thickness suggests that there is long-range attractive interaction between DNA molecules at higher spermidine concentrations. Rau and Parsegian have proposed that hydration forces underlie long-range attractive interactions between parallel DNA strands in the presence of condensing agents.³¹ Stabilization of strand-strand interactions is also suggested by the presence of flowers or disks on the top of larger aggregates, i.e., growth of condensates in the third dimension. Disks show another form of strand-strand stabilization. The thickness of the resolvable strands in a disk is clearly greater than individual strands seen in individual linear molecules or in flowers (e.g., point 2 in Figure 4E). This suggests that the strands in the disk are composed of at least two DNA molecules closely associated. The number of strands cannot be directly determined, although in some images it appears that two thin strands emerge from one thick one. Disks have never been seen in the absence of flowers in the same preparation, while flowers are frequently seen in the absence of disks. In addition, it appears in many

images that a disk is forming from a flower. Hence it is likely that disk formation follows flower formation.

Potential Problems. There are two primary types of artifacts that need to be considered in interpreting the data presented, sampling and drying. In almost all studies of the type presented here, there is a question of how well the composition of adsorbed structures represents the composition that is in solution. We have no readily accessible way of determining this, and hence, it is possible that there are intermediates in solution that are missed in this study. However, this does not significantly effect the interpretation of the data, since we report only on the structures that are seen and no assumptions about ones that are not. The question of how the substrate may affect the structure of the condensates is discussed below.

Drying artifacts is another concern that is shared with other studies, particularly ones based on negative stain electron microscopy. Our attempts to address this by directly visualizing the intermediates by AFM without drying have been unsuccessful to date. However, in examining the data, it is very difficult to see how drying would have contributed to the structures seen. To begin with, there are several unique structures with very different characteristics and any drying artifact would have to be a subtle function of spermidine concentration. Further, the effects of capillary forces on DNA adsorbed or attached to solid supports are typically quite dramatic, producing highly stretched molecules.^{32,33} Hence, while there are no obvious effects from drying and we feel that it is unlikely to have contributed significantly to the structures shown, it cannot strictly be ruled out.

Influence of Substrate on Observed Structures. The chemical environment at the liquid-solid interface is dramatically different than that of the bulk solution. Hence the effects of the substrate on the observed structures must be considered. The direct interaction of mica substrate with the DNA in the presence of spermidine must be attractive, or the DNA would not adsorb to the substrate. Making that assumption there are two limiting cases: either the DNA can rearrange after adsorption, or it is more or less immobile after adsorption (on the time scale of the experiment). If the DNA cannot rearrange, then the structures observed are collapsed forms of the structures in solution, and there is no direct effect of the substrate. If the DNA can rearrange, and the predominant interaction with the substrate is attractive, one would expect the crossovers to resolve themselves and DNA to lay flat on the surface, maximizing contact with the substrate. Therefore structures such as loops, flowers, and disks cannot be the result of a substrate-DNA interaction. The large aggregates that form at high spermidine concentration may on the other hand be significantly influenced by the substrate. The formation of these structures is evidence for stabilization between DNA molecules along their lengths, which should extend in all dimensions. However, the aggregates seen are highly planar. Such a planar morphology may result from the collapse of the three-dimensional aggregate onto the surface or may result from the attractive interactions between the DNA and substrate dominating those particular DNA-DNA interactions. In either case the interpretation that there is a stabilization between DNA molecules along their lengths is valid. All the arguments presented above suggest that the structures observed may be influenced by the substrate but are predominantly the result of DNA-DNA interactions and not DNA-substrate interactions.

(31) Rau, D. C.; Parsegian, V. A. *Biophys. J.* **1992**, *61*, 246.

(32) Bensimon, A.; Simon, A.; Chiffaudel, A.; Croquette, V.; Heslot, F.; Benimon, D. *Science* **1994**, *265*, 2096.

(33) Thundat, T.; Allison, D. P.; Warmack, R. J. *Nucleic Acids Res.* **1994**, *24*, 4224.

Pathways to Condensed DNA. The ability to define structural intermediates in a DNA condensation pathway raises the question of how many pathways there are and how many end points there are. For work in vitro the only well-defined end points are toroidal or rod-shaped DNA. These are known end points for spermidine-induced condensation in solution, and hence, they are the presumed end points for the spermidine-induced condensates described here. However, the inability to use high concentrations of spermidine and achieve these end point condensates in the system used leaves open the possibility that the intermediates we describe are not in the pathway to toroids or rods. If they are not, they represent intermediates (possibly including end points) in a condensation pathway for which the end points have not been characterized. It should be noted that the presence of a surface need not significantly interfere with DNA condensation, as it has been shown that surface-confined cations can prompt the formation of toroids with roughly normal dimensions.³⁴ In addition, it has been shown that protamines can induce the formation of toroids on mica surfaces.¹⁹

Thermodynamic and spectroscopic experiments have defined a major transition in the DNA condensation pathway as an abrupt collapse that occurs when approximately 90% of the backbone charges are neutralized by a condensing agent.³⁵ The recent work by Böttcher et al.²⁴ demonstrates a series of complex multimolecular condensates characterized by parallel bundles of DNA and frequent partial toroids, formed in the presence of spermine and uranyl acetate. Because these structures are highly condensed and have almost complete toroids they appear to be post-collapse structures and, hence, may be late intermediates. The existence of such structures is consistent with the idea that there is a slow post-collapse rearrangement of DNA into the final toroid or rod-shaped forms. In contrast, the intermediates described here are initially single molecules, in general are much more loosely associated, and therefore appear to be early “pre-collapse” intermediates.

Thermodynamic versus Kinetic Intermediates. The experiments presented were not designed to strictly test whether the intermediates presented are kinetic intermediates or ther-

(34) Fang, Y.; Hoh, J. H. *Nucleic Acids Res.* **1998**, *26*, 588.

(35) Manning, G. S. *Q. Rev. Biophys.* **1978**, *2*, 179.

modynamic intermediates. Rather we were interested in how stable the structures observed were over the experimental time scales typically used and, hence, how sensitive our results would be to variations in incubation times. The results show that, for the intermediates examined, changes are slow over the time scales used.

Other Considerations. The use of a surface to confine structures is a major difference between the work reported here and the bulk of the literature describing the thermodynamic, spectroscopic, and other solution characterizations of the cation-induced condensation process. This limits the direct comparisons that can be made between the data presented here and quantitative solution data. It also presents the inherent interpretation difficulties when collapsing a three-dimensional structure onto a two-dimensional surface. However, while it is difficult to deduce what the reported structures may have looked like in free solution, the structures observed are well defined and highly reproducible. In addition, in biological systems, there are many surfaces with which DNA can and does interact. One might even view the nucleosome as a surface onto which DNA “condenses.” Hence, while it remains an open question as to whether the intermediates described here are part of the pathway to “free” toroids or rods that have been well characterized, there is no apparent reason to think that this pathway is less important than the pathway that does lead to “free” toroids or rods (if they are in fact different).

Conclusion

The main result presented here is that there are intermediates early in spermidine-induced DNA condensation on mica that have unique structural features and are stable on the time scale of minutes to hours. The structures identified suggest that there are five steps in the process: reduction of apparent persistence length, loop formation, crossover stabilization, multimerization, and strand–strand stabilization.

Acknowledgment. This work was supported by in part by NIH Grant HGO1518 (J.H.H.). We thank Tom Spisz for assistance with computer programming for the data analysis.

JA981332V